



Controls on temporal patterns in phytoplankton community structure in the Santa Barbara Channel, California

Clarissa R. Anderson,¹ David A. Siegel,² Mark A. Brzezinski,³ and Nathalie Guillocheau²

Received 4 May 2007; revised 15 August 2007; accepted 10 October 2007; published 29 April 2008.

[1] Characterizing phytoplankton succession in the context of physical and chemical processes is important for understanding the mechanisms driving phytoplankton species composition and succession. An understanding of these processes ultimately influences the ability to predict the contribution of phytoplankton to carbon cycling, the initiation and persistence of harmful algal blooms, and the ability to use satellites for the remote sensing of specific phytoplankton taxa important for biogeochemistry. A statistical analysis of 5 years (1998–2003) of phytoplankton pigment concentrations from the Santa Barbara Channel using empirical orthogonal functions reveals four dominant modes of variability that explain 80% of the variance in the pigment data set. The annual cycle is characterized by a switching from a mixed-phytoplankton assemblage mode to modes dominated by either diatoms, dinoflagellates, or a combination of nano- and pico-phytoplankton. The dominant two modes correspond to a prebloom condition that precedes upwelling conditions, with all identified phytoplankton groups present in low abundance and a diatom-dominated upwelling state that develops following spring upwelling. In 2001, the EOF analysis indicated a transition toward more intense diatom blooms in spring and summer and fewer, large dinoflagellate blooms. This trend was corroborated by analyses of diagnostic pigments and CHEMTAX analysis and may be linked to an increase in local upwelling intensity between 2001 and 2003. Both spring diatom blooms occurring after 2001 were dominated by toxic *Pseudo-nitzschia* species and led to significant marine mammal deaths in the channel in 2003.

Citation: Anderson, C. R., D. A. Siegel, M. A. Brzezinski, and N. Guillocheau (2008), Controls on temporal patterns in phytoplankton community structure in the Santa Barbara Channel, California, *J. Geophys. Res.*, *113*, C04038, doi:10.1029/2007JC004321.

1. Introduction

[2] Phytoplankton biomass and productivity in the Santa Barbara Channel (SBC) are among the highest in the Southern California Bight [Mantyla *et al.*, 1995], supporting rich coastal ecosystems along the mainland coast and within the Channel Islands Marine Sanctuary [Beers, 1986]. Located at the northern extreme of the Bight, phytoplankton dynamics and species composition within the channel are influenced by a complex local circulation and by the interplay between seasonal freshwater runoff, upwelling at Point Conception to the west, local upwelling within the channel and the influx of relatively oligotrophic Southern California Bight waters from the east. As a result, phytoplankton biomass within the SBC shows a high degree of

variability on fairly small spatial scales of a few kilometers or less [Otero and Siegel, 2004].

[3] Studies of the phytoplankton community in the Southern California Bight show that spatial variations in overall phytoplankton biomass are often accompanied by dramatic shifts in species composition [Venrick, 1998]. Changes in species composition not only affect biogeochemical cycling and marine food webs, but can contribute a significant amount of variability to regional bio-optical estimates of primary production [Claustre *et al.*, 1997; Balch and Byrne, 1994]. For the SBC, recent attempts to reduce error in chlorophyll concentrations estimated from regionally tuned inversion models applied to water column optical properties have suggested phytoplankton community composition as a source of uncertainty [Kostadinov *et al.*, 2007]. An assessment of phytoplankton community structure and its changes would improve our ability to use ocean optics and satellite remote sensing to predict phytoplankton productivity and carbon cycling.

[4] The SBC is a nearshore, temperate basin at the confluence of the cool, fresh equatorward flow of the California Current and poleward flow of the warmer, saltier recirculation of the Southern California Bight [Lynn and Simpson, 1987]. Owing to this transitional location, the circulation of the SBC and its relationship with the

¹NOAA, ESSIC/CICS, University of Maryland, College Park, Maryland, USA.

²Institute for Computational Earth System Science, University of California, Santa Barbara, California, USA.

³Marine Science Institute and the Department of Ecology, Evolution, and Marine Biology, University of California, Santa Barbara, California, USA.

California Current System has been studied in great depth. [e.g., *Lynn and Simpson*, 1987; *Winant et al.*, 2003; *Harms and Winant*, 1998; *Chen and Wang*, 2000; *Breaker et al.*, 2003; *Oey et al.*, 2001], revealing a complex system of wind- and geostrophy-driven circulation states. Typically along the coast of California to the north of the SBC, equatorward winds drive Ekman transport over the continental shelf, supporting strong upwelling conditions for much of the spring and summer [*Winant et al.*, 1987, 2003]. From Point Conception at the west end of the SBC toward the Santa Barbara Channel Islands (Figure 1), these winds lose strength as they diverge from the transverse coastline. This leads to spatially variable wind fields and sea level gradients that are the main drivers of water circulation within the SBC [*Harms and Winant*, 1998]. Although seasonal upwelling is less frequent in the SBC relative to that along the central and northern California coasts, it does occur for brief periods along the mainland coast during spring [*McPhee-Shaw et al.*, 2007]. These events are often influenced by temporally variable eddies [*Harms and Winant*, 1998] to produce a patchy distribution of nutrients in time and space. Storm water runoff from local watersheds also drives water quality variability along the mainland of the SBC [*Mertes and Warrick*, 2001; *Warrick et al.*, 2004; *Otero and Siegel*, 2004]. All these factors are expected to significantly affect phytoplankton community dynamics and succession.

[5] The insights of local and regional studies by *Allen* [1922], *Orwig* [1978], *Goodman et al.* [1984], and *Venrick* [1998] gained through microscopic identification of species composition are indispensable to the new generation of studies based on coarser taxonomic groupings retrieved from rapid pigment analyses. Over the last decade, several researchers have explored methods for quantifying variability in phytoplankton production, biomass, and community structure solely from phytoplankton pigment concentrations [e.g., *Gieskes et al.*, 1988; *Siegel et al.*, 1990; *Letelier et al.*, 1993; *Moline and Prezelin*, 1996; *Claustre et al.*, 1997; *Vidussi et al.*, 2001; *Lohrenz et al.*, 2003]. A useful result of these approaches is the identification of basic biogeochemical components or functional groups from pigment data [*Vidussi et al.*, 2001]. Deriving quantitative taxonomic information from pigment markers, however, has not been a trivial task, particularly for those groups which share accessory pigment types or do not have obviously taxonomically unique marker pigments. *Mackey et al.* [1996] reduced much of this error with their matrix factorization program called CHEMTAX (CHEMical TAXonomy) for estimating algal class abundances from diagnostic pigments that employs a matrix of accessory pigment: chl *a* ratios to define different taxonomic groupings. CHEMTAX has been applied to different geographic regions with reasonable success and is often used in conjunction with microscopy and other multivariate statistical techniques [*Mackey et al.*, 1996; *Schlüter et al.*, 2000; *Lohrenz et al.*, 2003]. It is shown here that CHEMTAX functions as a useful approximation of patterns in large-scale, long-term studies where time and resources preclude microscopic identification.

[6] In this paper, we analyze a 5-year time series of phytoplankton pigment concentrations from the SBC determined by high-performance liquid chromatography (HPLC) to identify recurring phytoplankton assemblages and their relationship to seasonal changes in physical circulation and

nutrient abundance. The results show a fairly regular seasonal pattern of phytoplankton succession superimposed on a long-term increase in the intensity and frequency of diatom blooms during spring and summer. This change in the magnitude of diatom blooms in the channel coincides with an increase in the frequency of toxic diatom blooms in the SBC after 2001 that have caused several episodes of marine mammal deaths.

2. Methods

2.1. Data Collection

[7] Monthly to bimonthly cruises were conducted over a 5-year period (1998–2003) in the SBC as part of the UCSB Plumes and Blooms (PnB) project to study optical, physical, biological, and chemical properties along a seven-station, cross-channel transect from Santa Cruz Island to the mainland coast (Figure 1). The northern- and southern-most stations represent shallow locations on the continental shelf (45 and 75 m, respectively), while the remaining sites are in waters deeper than 250 m. This total distance of ~40 km was sampled in a single day on each cruise. Conductivity-temperature-depth (CTD) profiles were collected at each station with a Sea-Bird Electronics 911 plus CTD on an SBE32C compact rosette fitted with twelve 8-L Niskin bottles. This CTD was replaced in December 2000 by a similarly fitted Sea-Bird Electronics SeaCat Profiler. Surface water samples were collected at each station and at seven discrete depths between the surface and 75 m at the midchannel station (Station 4, Figure 1) for determination of concentrations of chlorophyll *a*, accessory pigments, dissolved inorganic nutrients, lithogenic silica and biogenic silica. All collection procedures are in accordance with the techniques recommended by the U.S. JGOFS and SeaWiFS programs [*Knapp et al.*, 1993; *Mueller and Austin*, 1995].

[8] Phytoplankton pigment concentrations were analyzed by HPLC in the CHORS laboratory of J.R. Perl and C.C. Trees at San Diego State University using methods proposed by NASA [*Bidigare et al.*, 2003]. After filtration of ~1 L surface water onto 0.7 μm Whatman GF/F 25 mm glass fiber filters each sample was frozen in liquid nitrogen. The filters were later extracted in 4 mL of 100% acetone containing an internal pigment standard (canthaxanthin) to correct for volumetric changes during extraction. An ODS-2 C18 column with a three-solvent gradient system and a ThermoQuest UV6000 scanning diode array absorption detector was used to separate and quantify pigments in each extract. Chlorophyll degradation products were detected and quantified with a ThermoQuest FL3000 scanning fluorescence detector. All system calibrations were performed using pigment standards from Sigma Chemical Co. and DHI, Institute of Water and Environment, Denmark.

[9] The pigments selected and their corresponding taxonomic associations are peridinin (dinoflagellates), fucoxanthin (diatoms), 19'-butanoyloxyfucoxanthin (chrysophytes, some haptophytes), 19'-hexanoyloxyfucoxanthin (haptophytes), prasinoxanthin (prasinophytes), violaxanthin (chlorophytes, including prasinophytes), alloxanthin (cryptophytes), lutein (chlorophytes), zeaxanthin (cyanobacteria), chlorophyll *b* (chlorophytes, prasinophytes); chlorophyll *a* and total chlorophyll represent total phytoplankton biomass. Prochlorophytes are not represented in the analysis

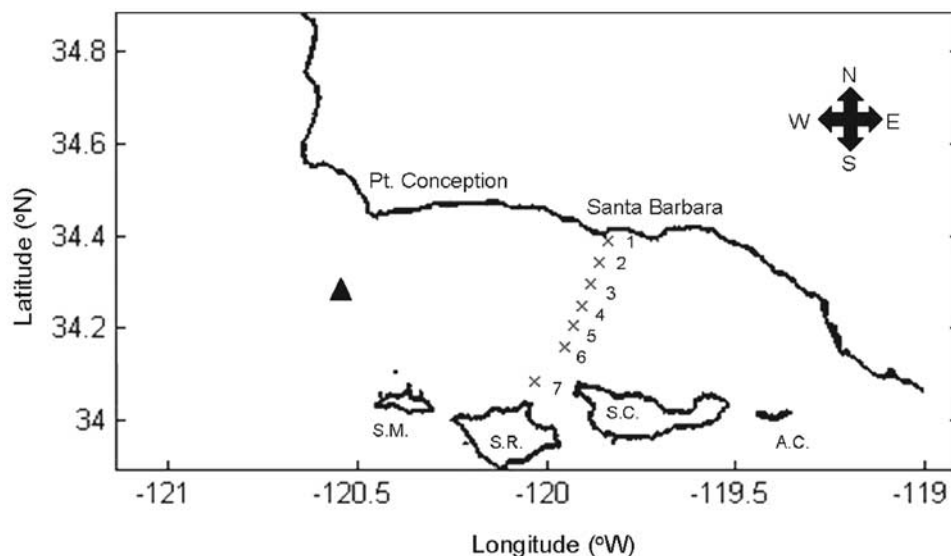


Figure 1. Map of the Santa Barbara Channel (SBC) and the Plumes and Blooms (PnB) study transect (crosses indicate station locations); solid triangle indicates location of NOAA buoy 46054. The SBC marks the northern boundary of the Southern California Bight and is itself bordered on the south by the Channel Islands. Station 1 is the northernmost station, located just off the coast of Santa Barbara, California. Station 7 is the southernmost station, located north of Santa Rosa Island. Stations 1–6 are separated by 3 nautical miles, and station 6–7 by 6 nm; all vertical profiles were taken from the midchannel station 4.

owing to analytical constraints in resolving the pigments monovinyl and divinyl chlorophylls *a* and *b*. This group is not expected to be important in surface waters of the SBC. Neoxanthin and anthoxanthin were not measured. Other accessory pigments such as the beta-carotenes, chlorophyll-*c* group, and the photo-protective diato/diadinoxanthins are insufficiently diagnostic of the major classes being assessed here, and therefore they were excluded from the analyses.

[10] Independent chlorophyll and phaeopigment analyses were performed with a Turner Designs 10AU digital fluorometer. A 250 mL seawater sample was filtered through a Whatman GF/F 25 mm glass fiber filters, which was immediately frozen in liquid nitrogen. Pigments were extracted in 90% acetone for ~36 hours at -20°C and fluorescence measured before and after the addition of two drops of 1.2 M HCl. Dissolved inorganic nutrient analysis was performed by the UCSB Marine Science Institute Analytical Lab using flow injection techniques on seawater collected in 20-mL plastic scintillation vials. Detection limits for nitrate (NO_3^-), ortho-phosphate (PO_4^-), and silicic acid ($\text{Si}(\text{OH})_4$) are $0.1 \mu\text{M}$, $0.05 \mu\text{M}$, and $0.2 \mu\text{M}$, respectively. For biogenic and lithogenic silica concentration analysis, 630 mL of seawater were filtered through a $0.6 \mu\text{M}$ polycarbonate membrane filter, dried at 60°C and processed using the serial NaOH/HF digestion developed by Brzezinski and Nelson [1989].

2.2. Data Analysis

[11] Variability within the 5-year HPLC phytoplankton pigment time series was examined using empirical orthogonal function (EOF) analysis, a statistical technique used to describe the spatial and temporal variability of a time series of data as orthogonal functions, termed modes, analogous to the axes in principal components analysis [e.g., Emery and

Thomson, 1997]. Where they differ is in the ability of the EOF method to reveal both spatial and temporal patterns in the original data set. We apply EOF analysis to surface concentrations of ten of the phytoplankton pigments from the monthly PnB cruises from 1998 to 2003 ($n = 474$ time points). Data are mean-centered and normalized with respect to the standard deviation prior to the analysis. EOF determines the fraction of the variance in the data set explained by each mode and provides an eigenvector of the relative amplitudes of each mode through time which reflects the contribution of each mode to the total variance in the data set at each point in time. The number of modes generated is the same as the number of pigments included in the analysis. Generally, the first several modes contain the majority of the variance and are most easily linked to potential environmental drivers.

[12] We compared each of the dominant EOF pigment modes with physical and chemical properties for interpretation of environmental forcings on the observed variability in phytoplankton community structure. Salinity (ppt), temperature ($^{\circ}\text{C}$), and the stratification index (m) are all CTD-derived. The stratification index is calculated according to methods described by Guzman-Bustillos *et al.* [1995] and is the average density difference per meter measured between 5-m depth intervals from the surface to 75 m. Monthly wind climatologies were assembled from the Santa Barbara West NOAA buoy 46054 (Figure 1), and data on the discharge of the Santa Clara River were obtained from USGS gauge 11114000. Wind speed, wind direction, and river discharge were computed as means for the eight days preceding each cruise. Monthly values of the Southern Oscillation Index (SOI) and of the Pacific Decadal Oscillation (PDO) indices were obtained from the websites <http://www.bom.gov.au/climate/current/soihtm1.shtml> and <http://jisao.washington>.

Table 1. Specifications for the Size Class and CHEMTAX Methods of Determining the Relative Abundance of Taxa in the Phytoplankton Community Using Diagnostic Pigments Selected for EOF Analysis^a

Diagnostic Pigments	Size-Class Groupings			CHEMTAX Groupings and Pigment Ratios							
	Taxon	Size	Group	CYANO	CHLOR	PRAS (T3)	CRYPT (T3)	HAPT (T3)	CHRYD	DINO	DIAT
Chlorophyll <i>a</i>	All		Total = S (All Pigments)	0.742	0.628	0.403	0.814	0.370	0.411	0.485	0.570
Zeaxanthin	CYANO	0–2 mm	Pico = [S (Zea + Chlb)]/Total	0.258	0.006	0.000	0.000	0.000	0.060	0.000	0.000
Chlorophyll <i>b</i>	CHLOR,PRAS	0–2 mm		0.000	0.165	0.381	0.000	0.000	0.000	0.000	0.000
Prasinolanthin				0.000	0.000	0.127	0.000	0.000	0.000	0.000	0.000
Lutein				0.000	0.127	0.004	0.000	0.000	0.000	0.000	0.000
Violaxanthin				0.000	0.035	0.025	0.000	0.000	0.087	0.000	0.000
Alloxanthin	CRYPT	2–20 mm	Nano = [S (Allo + 19'-HF + 19'-BF)]/Total	0.000	0.000	0.000	0.186	0.000	0.000	0.000	0.000
19'-HF	HAPT	2–20 mm		0.000	0.000	0.000	0.000	0.680	0.000	0.000	0.000
19'-BF	CHRYD	2–20 mm		0.000	0.000	0.000	0.000	0.012	0.152	0.000	0.000
Peridinin	DINO	>20 mm	Micro = [S (Perid + Fuco)]/Total	0.000	0.000	0.000	0.000	0.000	0.000	0.515	0.000
Fucoxanthin	DIAT	>20 mm		0.000	0.000	0.000	0.000	0.047	0.400	0.000	0.430

^aSize class groupings, “Pico,” “Nano,” and “Micro” plankton are adapted from *Vidussi et al.* [2001]. CHEMTAX pigment ratios are adapted from CSIRO guidelines [Mackey *et al.*, 1997] to better reflect regional flora, where Type 3 Prasinophytes contain prasinolanthin, and Type 3 Haptophytes represent prymnesiophyte algae that contain fucoxanthin, 19'-HF, and less 19'-BF than representatives of *Phaeocystis* spp. [Mackey *et al.*, 1997; Jeffrey and Wright, 1994]. Class abbreviations: CYANO, Cyanobacteria; CHLOR, Chlorophytes; PRAS, Prasinophytes; CRYPT, Cryptophytes; HAPT, Haptophytes; CHRYD, Chrysophytes; DINO, Dinoflagellates; DIAT, Diatoms (Bacillariophyceae).

edu/pdo, respectively. The chemical parameters used were dissolved ($\text{Si}(\text{OH})_4$, PO_4^{3-} , NO_3^- , NO_2^-) and particulates (biogenic and lithogenic silica). Correlation coefficients within 95% confidence limits were calculated for these selected variables and the dominant EOF mode amplitudes [Emery and Thomson, 1997]. The phytoplankton community composition at the extremes of each mode was also compared to the corresponding chemical and physical drivers of mode variability described above in order to relate changes in physical and chemical characteristics in the SBC to phytoplankton succession.

[13] To better understand the relationship between the amplitude time series for the dominant EOF modes and the potential physical and chemical factors that might drive the observed patterns, we identified cruise/station points corresponding to the extremes in the amplitude time series for each of the most significant modes. Histograms of the values of each amplitude time series were used to identify those cruises falling at the positive and negative extremes of each distribution. The number of cruise/station points selected for analysis was limited to those 30 that comprised the extremes of the positive (15 points) and negative (15 points) tails of each amplitude histogram. By constraining this analysis to the extremes of the amplitude function for each mode we maximize the ability to identify dominant abiotic drivers of variability within each mode. The use of a total of 30 points represents a 3% threshold on either tail of each distribution which is sufficiently restrictive to avoid low-magnitude amplitudes that do not represent extremes in the expression of each mode. Given the lack of normality in the amplitude frequency distributions, mean physical and chemical properties corresponding to the extreme upper and lower amplitudes were compared using the nonparametric, two-tailed Wilcoxon-Mann-Whitney (WMW) test. Variables that exhibited significant changes between the positive and negative extremes of each mode were identified as possible drivers of the mode's variations.

[14] We quantified the relative contributions of individual phytoplankton taxonomic groups to the extremes of each EOF mode using two methods. The first was the diagnostic pigment method of *Vidussi et al.* [2001], which can be used

to identify phytoplankton taxa by size class according to the relative abundance of seven diagnostic pigments: cyanobacteria, chlorophytes, and prasinophytes (corresponding to zeaxanthin, chlorophyll-*b* concentrations, respectively) represent the pico-plankton (0–2 μm); cryptophytes, haptophytes, and chrysophytes (corresponding to alloxanthin, 19'-hexanoyloxyfucoxanthin, 19'-butanolyoxyfucoxanthin concentrations, respectively) represent the nano-plankton (2–20 μm); dinoflagellates and diatoms (corresponding to peridinin, fucoxanthin concentrations, respectively) represent the micro-plankton (>20 μm). Total biomass was calculated as the sum total of the concentrations of these seven, nonredundant diagnostic pigments, while the relative abundance of the three size classes was calculated as the proportion of each summed subset to the total (Table 1). We exclude picoplanktonic prochlorophytes from our analysis because of the uncertainty of the requisite diagnostic pigments in the HPLC analysis and the relative unimportance of this group in the SBC.

[15] The second technique used for estimating the phytoplankton assemblage represented by the extremes of each mode was the CHEMTAX approach developed at CSIRO laboratories [Mackey *et al.*, 1996] for partitioning the pigment HPLC data into taxonomic groupings and quantifying their contributions to total biomass. This technique employs an iterative method of factor analysis to solve the least squares equation given by the inputs of raw HPLC pigment data and diagnostic pigment ratio information for each of the major phytoplankton groups of interest. From this series of optimizations, an estimation of the contribution of each phytoplankton class to the total chlorophyll in the sample is derived. For more information on the methods used in the CHEMTAX analysis, see Table 1 and Appendix A.

3. Results

3.1. Water-Mass Properties

[16] Water mass properties in the PnB time series show regular seasonal cycles, with pronounced interannual variability. The mean sea surface temperature (SST) over the 5-year period is 15.1°C. Maximum temperatures (> 19°C)

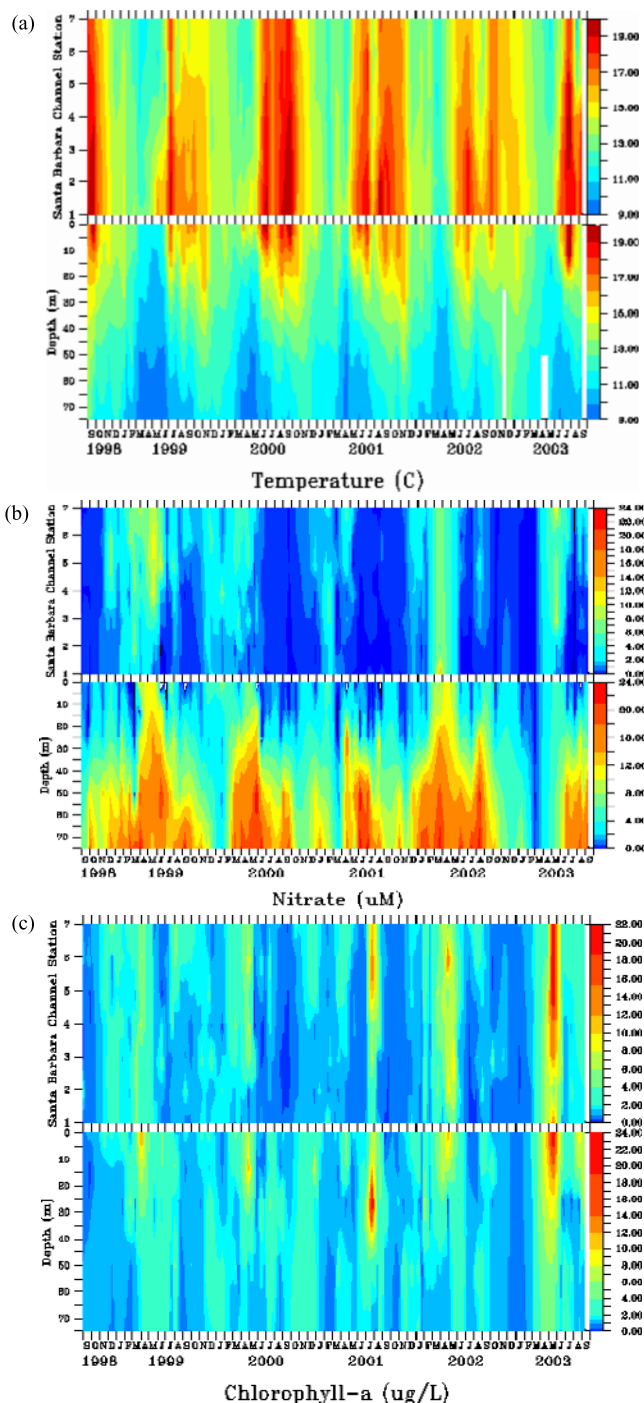


Figure 2. Time-station contours of (a) temperature ($^{\circ}\text{C}$), (b) nitrate (μM), and (c) chlorophyll *a* ($\mu\text{g L}^{-1}$) along the seven-station PnB transect from September 1998 to August 2003. Vertical profiles (0–75 m) were taken at station 4 only (Figure 1). Gaps in contours are due to instrument failure.

occurred during summer months in 2000 and during the 1998 El Niño summer when warm, tropical water masses were present in the Santa Barbara Channel (Figure 2a). Coldest temperatures occurred during winter and also during spring when local upwelling brought cold, saline

water to the surface (Figure 2). The lowest SSTs in the record ($< 12^{\circ}\text{C}$) were during the 1999 La Niña year and again in 2002 and 2003, associated with intense upwelling that brought nitrate-rich waters to the surface across much of the SBC (Figure 2b).

[17] Nutrient distributions also show marked seasonal variation and significant, primarily ENSO-related, interannual variability. Surface nitrate concentrations (mean = $1.5 \mu\text{M}$, Figure 2b) rose to over $10 \mu\text{M}$ during spring upwelling, but were also high for brief periods in early summer. The highest surface nitrate concentrations ($10\text{--}12 \mu\text{M}$) are observed during the spring of the 1999 La Niña year and the spring of 2002 and 2003, consistent with the colder surface temperatures during those periods. In contrast, nitrate concentrations were much lower ($0.5\text{--}3 \mu\text{M}$) during the springs of 2000 and 2001 when warmer temperatures suggest less intense upwelling (Figure 2a). Summer-time nitrate concentrations were below detection during all years. During the La Niña summer of 1999, these minima were restricted to the nearshore stations, seemingly a result of the particularly high nitrate concentrations at offshore stations in the preceding months.

[18] Chlorophyll concentrations reached high values in the springs of 2002 and 2003, and during July–August of 2001 (Figure 2c). During these periods, chlorophyll-*a* concentrations in excess of $8 \mu\text{g L}^{-1}$ were present throughout the upper 20 m of the water column. Those values are considerably higher than typical concentrations found in the Southern California Bight [Mullin, 1986; Venrick, 1998]. These biomass peaks appear to be a response to intense upwelling in 2002 and 2003 as revealed by the nitrate and temperature distributions, but for the summer of 2001, we do not see a concomitant upwelling signal to match the high chlorophyll concentrations. In fact, recorded nitrate concentrations for this period do not exceed $0.3 \mu\text{M}$ (Figure 2b). It is likely that this summer phytoplankton bloom, which was mostly present at stations near Santa Cruz Island, was advected into the SBC from upwelled waters north of Pt. Conception rather than being the result of local upwelling. SeaWiFS and AVHRR imagery from early July 2001 seem to corroborate such a scenario whereby cold, high-biomass waters were advected from Pt. Conception into the western SBC. This is in contrast to the prolonged chlorophyll-*a* minimum associated with the 1999 La Niña year when advection of warm Southern Bight waters appeared to suppress primary production in the SBC [Otero and Siegel, 2004].

3.2. Variability in Accessory Pigment Distributions

[19] The surface distributions of three major carotenoid pigments, fucoxanthin, peridinin, and 19'-butanoyloxy-fucoxanthin, observed over the 5 years reflect changes in the physical and chemical properties described above (Figure 3). The distribution of the diatom diagnostic pigment, fucoxanthin, parallels peaks in chlorophyll, with high concentrations during spring followed by generally smaller, more sporadic blooms during the summer months (Figure 3a). This is not the case for 2001, however, when the spring diatom bloom was very weak with a larger and more persistent bloom occurring during summer, as observed with chlorophyll *a* (Figure 2c). During the 2002 and 2003 upwelling seasons, surface fucoxanthin concentrations

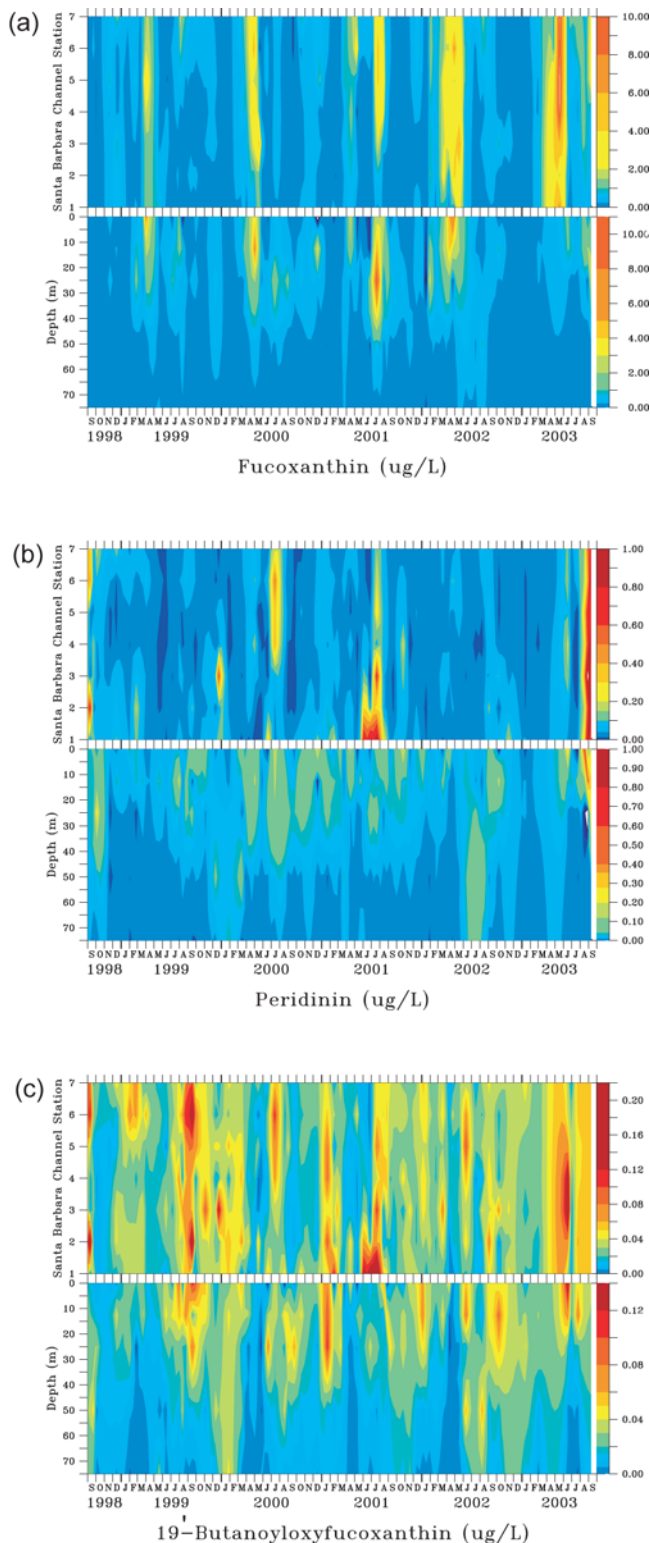


Figure 3. Time-station contours of selected diagnostic phytoplankton pigments sampled along the PnB transect from September 1998 to August 2003. (a) Fucoxanthin = diatoms, (b) peridinin = dinoflagellates, and (c) 19'-butanoyloxyfucoxanthin = haptophytes + chrysophytes. Note that the surface fucoxanthin concentrations from May 2003 were measured at 3–4 m on a separate SBC-LTER cruise.

remained high for several months, paralleling a similar trend in total chlorophyll-*a* biomass (Figure 2c). The high surface fucoxanthin concentrations observed during the spring of 2003 ($>10 \mu\text{g L}^{-1}$) were measured from waters collected between 3 and 4 m depth (Figure 3b) on a separate Santa Barbara Coastal–Long Term Ecological Research (SBC-LTER) cruise and are the highest in the record.

[20] Peridinin, the diagnostic pigment for dinoflagellates, is not present in concentrations nearly as high as those for fucoxanthin in the time series (Figure 3c). The highest peridinin concentrations ($\sim 0.9 \mu\text{g L}^{-1}$) occurred during summer periods and have relatively weak subsurface signatures compared to the other major diagnostic pigments (Figure 3). Peridinin concentrations peak in 2000 and 2001. The peak in 2001 was predominantly constrained to inshore stations, coincident with the more offshore and vertically extensive maxima in fucoxanthin during those same months (Figure 3b). Interestingly, the timing and spatial distribution of the nearshore maxima during the large 2001 bloom is mirrored in the distribution of 19'-butanoyloxyfucoxanthin (hereafter abbreviated 19'-BF; Figure 3c), a characteristic pigment of the chrysophytes. This class includes the silicoflagellates and is distinct from the haptophytes which produce both 19'-BF and 19'-hexanoyloxyfucoxanthin (hereafter abbreviated 19'-HF). In the SBC, peaks in relative chrysophyte abundance are generally late spring and summer events that often extend >30 m into the water column (Figure 3c) and display a great deal of overlap with dinoflagellate blooms (Figure 3b), an observation which will become important in the interpretation of the EOF results.

3.3. Modes of Phytoplankton Variability

[21] EOF analysis of the surface-layer time series of HPLC pigment concentrations offers a more comprehensive view of changes in phytoplankton composition. The first four EOF modes describe 80% of the total variance in the HPLC pigment data set and are easily related to environmental parameters. The fifth and successive modes account for $<6\%$ of the variance each and are not discussed further. The first EOF mode accounts for 38% of the variance (Figure 4) and is positively correlated with all pigments used in the analysis. There is a strong correlation between the first mode and the flagellate groups prasinophytes, chlorophytes, haptophytes, and cryptophytes, which contain the accessory pigments prasinoxanthin ($r^2 = 0.64$), chlorophyll *b* ($r^2 = 0.67$), violaxanthin ($r^2 = 0.42$), 19'-HF ($r^2 = 0.60$), and alloxanthin ($r^2 = 0.44$), respectively. The poor correlations between this mode and both the diatom diagnostic pigment fucoxanthin ($r^2 = 0.19$) and chlorophyll *a* ($r^2 = 0.38$) suggest that this mode represents prebloom conditions within the channel. The spatial and temporal distributions of the amplitude function for this mode (Figure 5) are consistent with such an interpretation since amplitudes are highest in spring and early summer prior to the major phytoplankton bloom episodes.

[22] Correlation analyses between the amplitude function of the first EOF mode and surface water properties also support the prebloom characterization. Significant correlations with higher salinities, low sea surface temperature, and high nutrient concentrations (Table 2) suggest this mode is related to upwelling of subsurface waters to the surface.

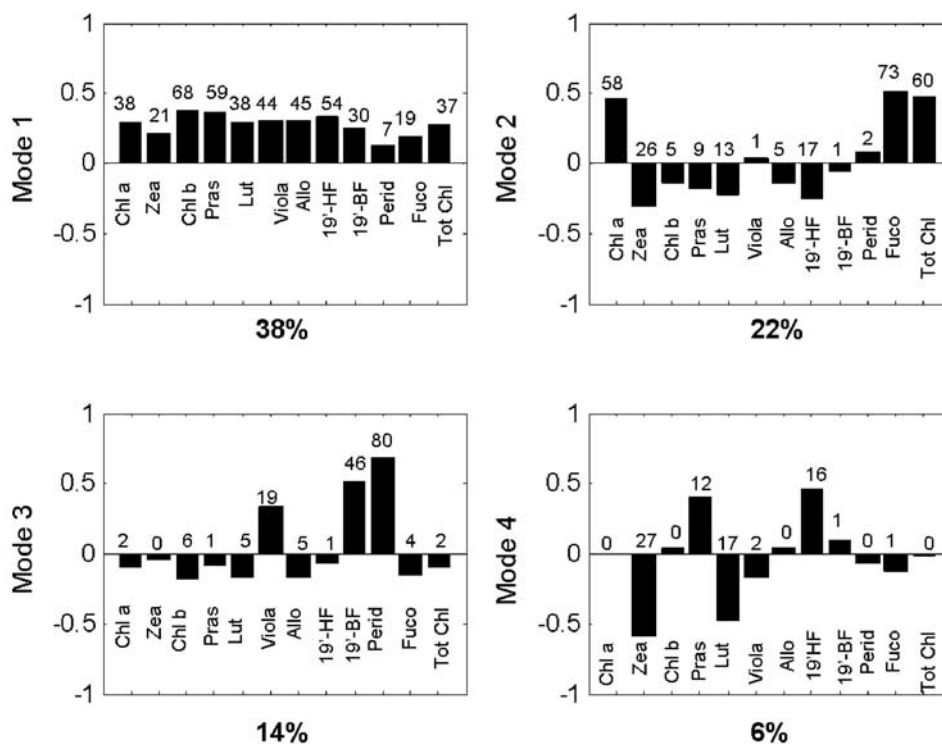


Figure 4. First four empirical orthogonal function (EOF) modes for eleven diagnostic phytoplankton pigments measured from September 1998 to August 2003 ($n = 474$). The values in bold, below each plot, represent the proportion of total variance explained by each mode. Numbers above each bar are the R^2 values between each pigment and the respective EOF mode. Pigment abbreviations denote the following: chlorophyll *a*, zeaxanthin, chlorophyll *b*, prasinoxanthin, lutein, violaxanthin, alloxanthin, 19'-hexanoyloxyfucoxanthin, 19'-butanoyloxyfucoxanthin, peridinin, fucoxanthin, and total chlorophyll.

Further, the absence of a significant correlation with biogenic silica combined with a positive correlation with silicic acid concentrations (Table 2) supports the conclusion that this mode is strongest prior to significant increase in diatoms.

[23] When the positive and negative extremes in the amplitude frequency distributions for the first EOF mode were mapped in time and space (Figure 6), the positive extremes occurred during spring and/or early summer of every year except 2001 and at stations 1 and 3 in December 1999 (Figure 6). Extreme amplitudes for the first mode are uniquely expressed without overlap with the extremes in the amplitude of any other mode at only four cruise/station points during the time series: 13 March 2000 (station 4); 17 June 2003 (stations 3–5). Thus, the phytoplankton assemblage at either extreme is influenced by this overlap with other modes. The differences between physical and chemical properties at the extreme amplitude end points for mode 1 show that the positive extremes of this mode are associated with high salinity, low temperatures, increased river discharge, and enhanced nutrient concentrations (Table 3). Additionally, the stratification index is significantly reduced for the positive compared to the negative extremes (Table 3), further supporting the association of this mode with upwelling.

[24] The application of CHEMTAX to the extreme upper and extreme lower third percentile amplitudes for mode 1 gave results that generally agreed with our interpretation of

mode 1 being a prebloom or early upwelling state. Quantification of the mean assemblage composition at the positive extremes yields 49% micro-plankton and ~50% nano/pico-plankton when grouped by chemotaxonomic size class (Figure 7a), which appears to contradict the fairly weak relationship between the micro-plankton pigment fucoxanthin and the first mode. When grouped using CHEMTAX factor analysis, 35% of the mean biomass at the positive extremes is attributable to diatoms (Figure 7a), despite the fairly low correlation between fucoxanthin and the first mode amplitudes ($r^2 = 0.19$). This is clearly due to the fact that as a prebloom state, the first mode often partially overlaps in time with the second mode which, as explained below, is dominated by diatoms. Prasinophytes and haptophytes contribute another 38% to the total mean biomass (Figure 7a) for the first mode extremes, in agreement with the dominant pigment structure for this mode (Figure 4). With diatoms comprising a third or more of the phytoplankton assemblage, we did not expect the significantly low biogenic silica concentrations observed at the positive extremes (Table 3). However, if this mode occurs most strongly at times when the phytoplankton population is just beginning to respond to upwelling conditions, it may be that the rise in diatoms seen in the CHEMTAX results represents initial increases in diatom growth rates prior to the accumulation of biogenic silica.

[25] The second EOF mode describes 22% of the variance and represents a diatom-bloom mode (Figure 4) with a

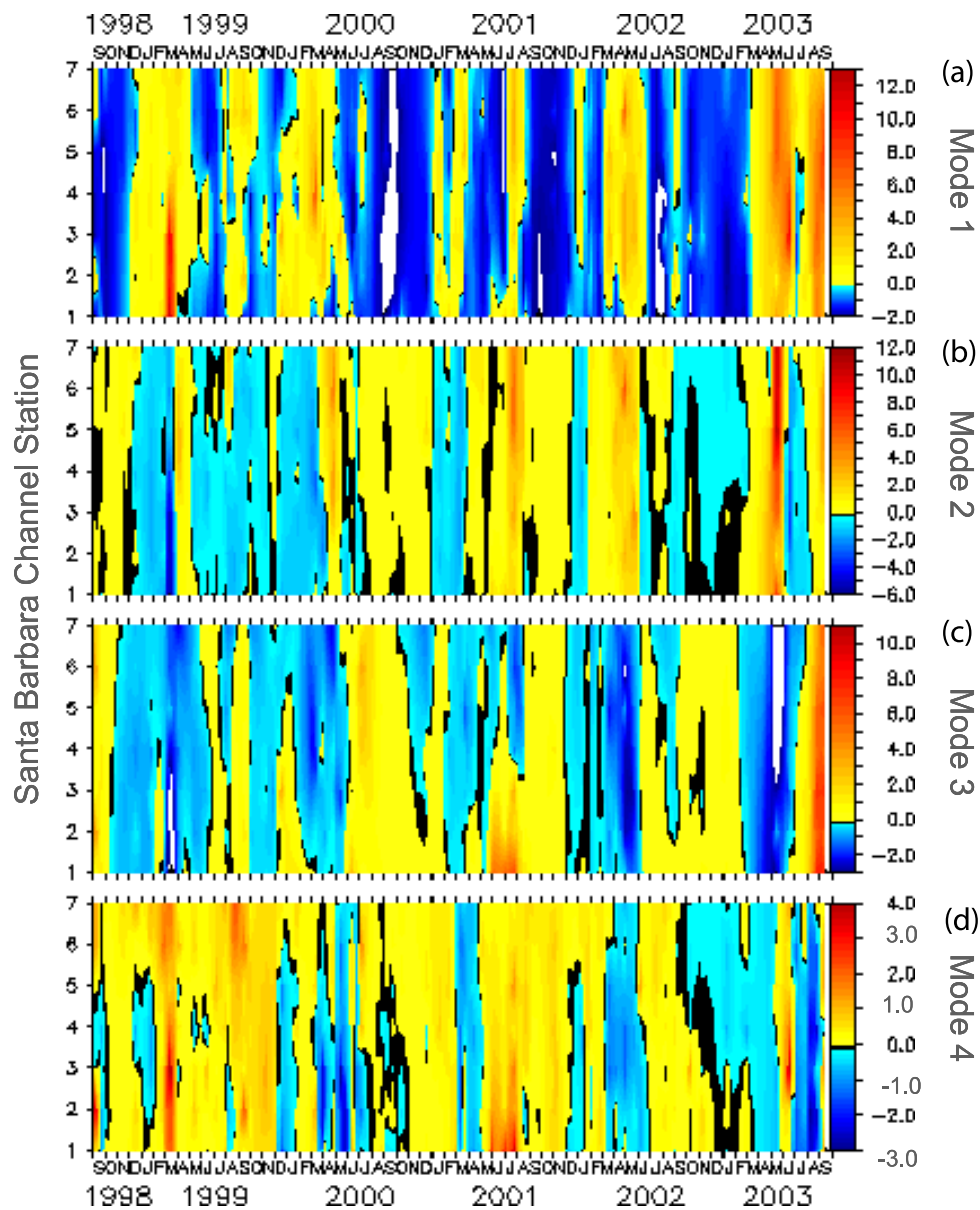


Figure 5. Time-station contoured distributions of the EOF amplitude time series for the four most significant modes. Station 7 is the most southern and offshore location. Note that amplitude signs for Mode 3 have been reversed to show peridinin (dinoflagellate) increases as positive (red) amplitudes.

strong positive correlation to fucoxanthin ($r^2 = 0.73$) and chlorophyll *a* ($r^2 = 0.58$). All other phytoplankton accessory pigments are inversely related or show a very weak positive correlation with this mode, consistent with it being predominantly diatom-driven. The spatial and temporal distribution of the amplitude factors shows strongest positive amplitudes in the summer of 2001 and the springs of 2002 and 2003 (Figure 5). The latter two diatom blooms appear to be a response to intense upwelling conditions as noted in the discussion of temperature and nitrate distributions (Figures 2a and 2b). In summer 2001, however, local upwelling may have been less important than advection in driving diatom bloom formation, as noted earlier for total chlorophyll biomass and evidenced in satellite imagery.

[26] Correlation analyses between the second EOF mode amplitude factors and in situ water properties support the

role of upwelling in the regulation of the diatom-dominated mode as a whole. A significant relationship with high wind speeds, high salinity, and low temperatures is observed for the second mode, but unlike with the first EOF mode, the temperature relationship is somewhat weaker and may indicate that this mode is associated with the warming of upwelled surface waters (Table 2). There is also a negative association with discharge from the Santa Clara River (see Figure 1), corroborating previous findings that runoff events do not play a major role in driving local phytoplankton blooms [Otero and Siegel, 2004]. As expected, biogenic silica is strongly correlated ($r = 0.60$) with the second mode, and to a lesser extent, low silicic acid supply and lower Si: P ratios (Table 2). This supports the idea that the second pigment mode reflects a springtime, diatom bloom state

Table 2. Correlation Coefficients (r) With $n-2$ Degrees of Freedom (DF) and 95% Confidence Limits for the Major Phytoplankton Pigment EOF Modes and Discrete Surface Water Properties

Correlation Coefficients (r)	EOF Mode 1 38%	EOF Mode 2 22%	EOF Mode 3 14%	EOF Mode 4 6%	DF
Salinity	0.182	0.26			405
Temperature	-0.392	-0.195	0.274	-0.243	407
Stratification Index			0.303	-0.183	317
Wind Speed		0.191			368
SOI		-0.13	-0.137		450
PDO	0.167		-0.222	-0.157	450
SC River Discharge		-0.182		-0.148	377
PO ₄	0.27		-0.191	0.189	440
Si(OH) ₄	0.346	-0.176	-0.215	0.166	440
NO ₃	0.292		-0.213	0.23	406
NO ₂	0.225				397
Biogenic Si		0.598			374
Lithogenic Si					374
Si:N				-0.136	396
Si:P	0.193	-0.322			439

when temperatures are reduced and uptake of inorganic nutrients is expected to be rapid [Dugdale *et al.*, 1990].

[27] The upper 3% positive amplitudes for mode 2 do not occur until the spring and summer months of 2000 through 2003, with unique expression at 9 cruise/station points across stations 3–7 during these years (Figure 6a). Both the size class and CHEMTAX groupings for the extreme positive amplitudes predict an assemblage comprised almost entirely

of diatoms (Figure 7b). WMW test results show significantly increased salinity, reduced silicic acid concentrations, and increased biogenic silica concentrations between the negative and the positive extremes (Table 3), in agreement with the correlation analysis for all amplitudes and consistent with the extremes of mode 2 being associated with upwelling-related diatom bloom events. Both the integrated fucoxanthin values (Figure 3a) and the amplitude time series for mode 2

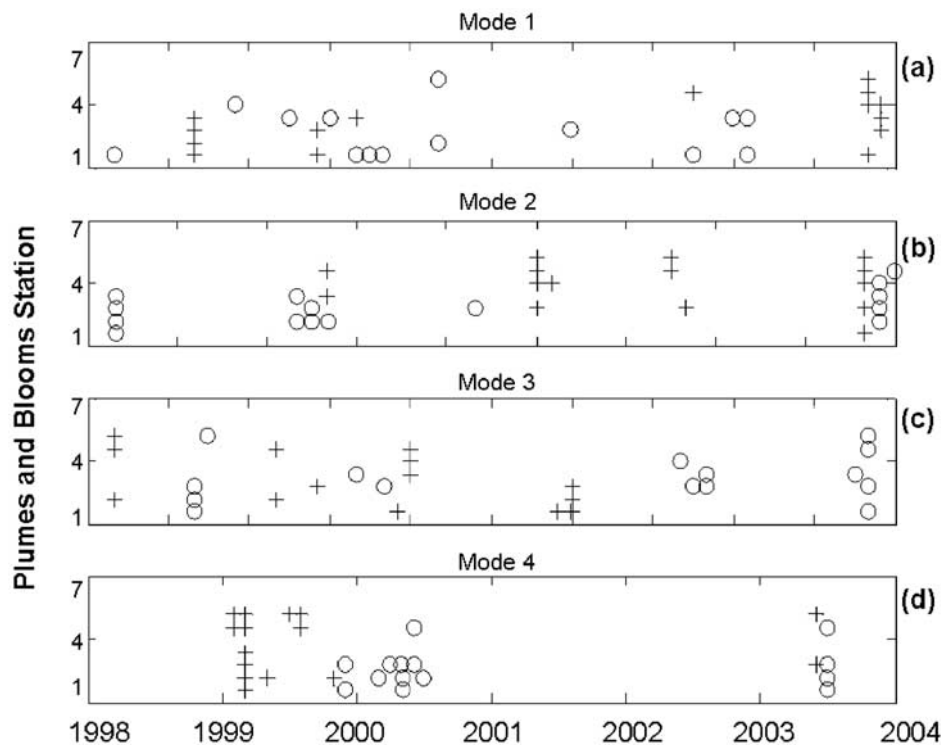


Figure 6. Cruise/station points for the upper 3% positive (pluses) and 3% negative (circles) amplitudes for EOF pigment modes 1–4. The number and spatial extent of extreme positive points for the third (diatom) and fourth (dinoflagellate) modes appear inversely related over the study period. Positive extremes for the fourth mode represent a nanoflagellate-dominated community, and negative extremes represent a more picoplankton-dominated community.

Table 3. Mean Values of Selected Physical and Chemical Parameters Evaluated for the Upper 3% Positive and Negative EOF Mode Amplitudes With the Correspondent Wilcoxon-Mann-Whitney (WMW) Test Results^a

	Mode 1				Mode 2				Mode 3				Mode 4			
	Pos.	Mean	Neg.	Mean N p-Value	Pos.	Mean	Neg.	Mean N p-Value	Pos.	Mean	Neg.	Mean N p-Value	Pos.	Mean	Neg.	Mean N p-Value
Salinity	33.72	33.58	27	0.004	33.75	33.65	27	0.028	33.62	33.77	24	0.000	33.67	33.59	26	n.s.
Temperature	12.65	15.74	27	0.001	13.04	13.72	27	n.s.	16.56	12.46	24	0.000	13.30	16.86	26	0.000
Stratification	0.06	0.10	20	0.005	0.05	0.07	17	n.s.	0.29	0.05	14	0.001	0.05	0.12	25	0.000
Wind Speed	6.38	7.25	25	n.s.	8.51	6.98	23	n.s.	7.81	6.52	18	n.s.	7.52	6.86	28	n.s.
SOI	0.08	2.81	30	n.s.	-4.19	4.72	28	0.012	1.23	1.22	28	n.s.	4.67	4.16	30	n.s.
PDO	0.07	-0.71	30	0.043	-0.15	0.28	28	n.s.	-1.10	0.10	28	0.000	-0.48	0.03	30	0.040
SCR Discharge	2.96	1.69	21	0.031	0.55	3.05	18	n.s.	0.15	3.82	15	0.019	0.33	0.15	28	n.s.
PO ₄	0.48	0.32	30	0.029	0.37	0.45	28	n.s.	0.22	45	28	0.007	0.43	0.23	29	0.002
Si(OH) ₄	5.80	3.24	30	0.037	2.70	5.96	28	0.006	1.65	5.48	28	0.040	6.20	2.06	29	0.000
NO ₃	3.50	1.64	24	0.004	0.94	2.85	22	0.017	0.64	5.00	22	0.000	4.06	0.69	30	0.000
NO ₂	0.17	0.09	24	0.005	0.10	0.15	22	n.s.	0.09	0.16	22	n.s.	0.15	0.10	30	0.018
BSi	0.37	1.18	23	0.015	9.17	0.62	18	0.002	0.82	3.31	20	n.s.	0.67	1.76	30	n.s.
LSi	0.50	1.08	23	n.s.	0.46	0.23	18	0.039	0.59	0.41	20	n.s.	0.40	0.40	30	n.s.
Si:N	2.17	4.07	24	n.s.	2.34	5.80	22	n.s.	4.41	1.71	22	n.s.	2.18	1654.96	29	0.040
Si:P	11.42	6.90	24	0.029	5.06	12.95	22	0.000	6.78	10.19	22	n.s.	13.49	10.09	29	0.020

^aHere n.s. indicates absence of a statistical difference between means at $\alpha = 0.05$. N is the sample size for each comparison and is equivalent to the degrees of freedom.

(Figures 5b and 6b) reveal an increase in the magnitude and extent of diatom blooms over the course of the time series (Figure 6b).

[28] The third EOF mode accounts for 14% of the variance in the pigment time series and correlates most strongly with the dinoflagellate diagnostic pigment, peridinin (Figure 4). The variance in the nanoflagellate accessory pigments 19'-BF and violaxanthin are together explained by an amount comparable to that of peridinin, while the remaining phytoplankton pigments correlate very weakly with the third mode and are inversely related to the previous three accessory pigments. The third mode could thus be described as a primarily dinoflagellate-driven state, secondarily forced by chrysophytes when total biomass is low and other net phytoplankton such as diatoms are rare or absent (Figure 4).

[29] The spatial and temporal distribution of the amplitude function for the dinoflagellate-bloom mode is presented in Figure 5c and shows peaks during summer both near the islands at stations 4–7 in 2000 and inshore near the mainland at stations 1–3 in 1998 and 2001. A third smaller peak in mode amplitude in December 1999 is also confined to the mainland continental shelf and is potentially due to nutrients supplied by storm runoff [Otero and Siegel, 2004]. Consistent with the interpretation of the third EOF mode as a dinoflagellate-bloom mode is a negative correlation with temperature and increased stratification (Table 2). The lack of a relationship with river discharge (Table 2) is unexpected, however, given the established link between runoff and some dinoflagellate blooms [e.g., Cembella et al., 2002; Doblin et al., 1999]. Overall, the results of the correlation analysis for the third pigment mode describe a dinoflagellate-dominated state that occurs under stratified conditions in nearshore, warm, low-nutrient waters primarily during summer months.

[30] The extreme positive amplitudes for the third mode, which correspond to higher dinoflagellate abundances (Figure 7c), are associated with lower salinities, high temperature, increased stratification, reduced river discharge, and low nutrient concentrations, particularly phosphate and nitrate (Table 3). Taken together, the correlation

and WMW analyses clearly associate the third mode with dinoflagellate dominance during warm, stratified, oligotrophic conditions in the absence of major storm events. In the one instance when these dinoflagellate-favorable conditions coincided with a midchannel diatom bloom in July 2001, dinoflagellates comprised only 18% of the phytoplankton community according to CHEMTAX and were isolated to the most nearshore stations (Figures 5 and 6c).

[31] The last EOF mode we consider describes 6% of the surface pigment variability and is driven by an alternating pattern of nano- and pico-phytoplankton abundance. The nano-phytoplankton component comprises haptophytes (19'-HF) and prasinophytes (prasinolaxanthin), while the pico-phytoplankton component is comprised mainly of cyanobacteria (zeaxanthin) and chlorophytes (zeaxanthin, lutein) (Figure 4). When the fourth EOF mode amplitudes are positive, haptophytes and prasinophytes are present in greater abundance, and when modal amplitudes are negative, the smaller chlorophytes and cyanobacteria dominate the mode (Figures 7d and 7e). The amplitude function of the fourth mode shows how these two assemblages vary in time and space with the positive peaks in amplitude corresponding to a higher abundance of haptophytes and prasinophytes and with extreme negative values indicating a greater relative abundance of chlorophytes and cyanobacteria (Figures 6d, 7d, and 7e). Positive expression of the mode is restricted to the winter and springs of 1999 and 2003. Negative amplitudes occur as sporadic, nearshore events throughout 2000 and again in the summer of 2003.

[32] Negative correlations between the amplitude factors for the fourth mode and indices of temperature, stratification, and Santa Clara River discharge suggest that haptophytes and prasinophytes are favored by colder, more mixed conditions in the absence of runoff events (Table 2). Increased nutrient loading is also an important driver for selection of the fourth mode positive amplitudes (Table 2). Conversely, the chlorophyte/cyanobacteria assemblage is negatively correlated with nutrient concentrations and positively correlated with temperature and stratification. Slightly higher silicic acid concentrations during these latter "blooms" appears to drive the overall negative relationship

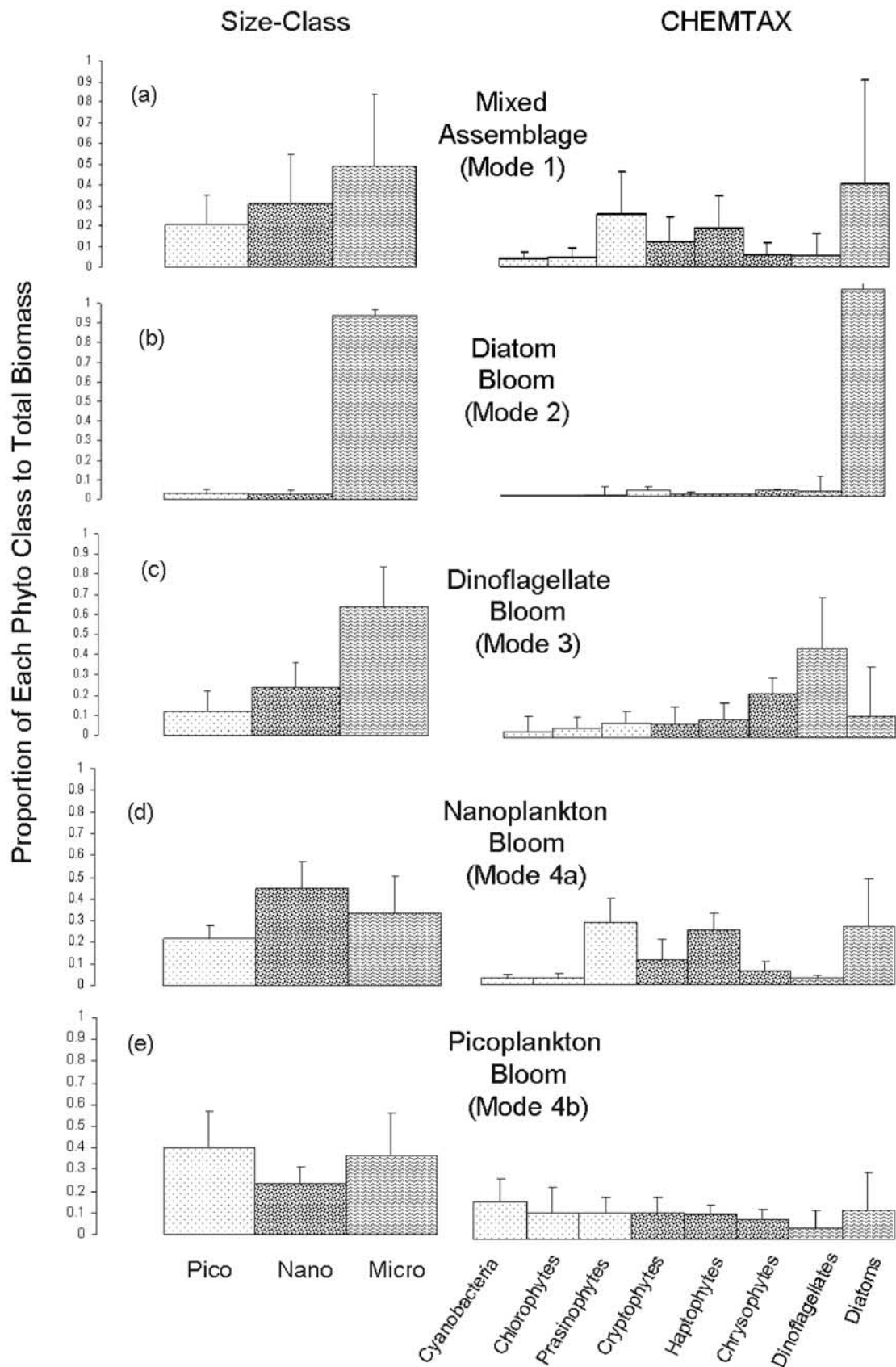


Figure 7

observed for the fourth mode and the Si:N ratio (Table 2). In summary, we find the fourth EOF pigment mode to describe two alternate flagellate assemblages separated in time and space by their opposing tolerances.

[33] The extremes for mode 4 better define the selective factors for these opposing nano- and pico-plankton assemblages. Favorable conditions for prasinophytes and haptophytes occurred in all seasons during 1999 at predominantly offshore stations, while those favoring cyanobacteria occurred mostly at stations 1–3 throughout the spring and summer of 2000 (Figure 6d). The WMW test comparing the positive and negative extremes confirms the results of the correlation analysis that the extreme amplitudes favoring nano-phytoplankton are associated with cooler, nutrient-replete, less stratified waters, while the extreme amplitudes favoring pico-phytoplankton are expressed during warm, stratified, fairly oligotrophic conditions (Tables 2 and 3). Both sets of conditions arose at two separate times in the summer of 2003 just following the large spring diatom bloom, which suggests that this mode represents two types of transition states which may either resemble the prebloom community of the first mode or represent a postbloom relaxation event when surface waters are warm and nutrient-poor.

4. Discussion

[34] Over the 5 years studied here, an EOF analysis revealed four dominant pigment states that describe the majority of the variability in phytoplankton pigment composition for the SBC. These modes consisted of distinct phytoplankton assemblages whose temporal patterns of abundance each displayed a unique relationship to the annual cycle of physical and chemical changes within the SBC. In other words, as the relative abundance of diagnostic pigments continuously fluctuates, there are a relatively small set of recurrent environmental conditions that are favorable for the growth and reproduction of specific taxa.

4.1. Controls on Seasonal Succession

[35] According to *Margalef* [1962, 1978] the flux of nutrients within aquatic systems regulates phytoplankton succession, while the frequency of water column destabilization is important for resetting the successional trajectory. Results from the EOF decomposition of phytoplankton pigments in our study provide evidence of significant switching from a mixed-assemblage mode to modes dominated by diatoms, dinoflagellates, and nano- or pico-plankton on seasonal timescales (Figure 8). Comparisons to physical and chemical properties suggest these modes represent: the onset of upwelling, post upwelling, oligotrophic-stratified, and transition states, respectively. Figure 8 shows a clear seasonal transition from dominance by the mixed-assemblage mode to the diatom- and dinoflagellate-dominated modes, with the two flagellate assemblages of the fourth mode alternating in dominance throughout the year. The transition

from the diatom to the dinoflagellate mode corresponds to a shift from cold, high-biomass waters to relatively warm, low-biomass waters (Figure 8).

[36] From the correlation analyses, it appears that reduced stratification of the water column (Table 3) initiates the mixed assemblage mode community, much like the first stage of *Margalef's* model of succession. This first EOF mode is comprised largely of flagellates and diatoms favored by unstratified, cold conditions. With the onset of seasonal stratification and the uptake of nutrients in surface waters, diatoms are expected to dominate the second stage community [*Margalef*, 1962; *Smayda*, 1963], and indeed our diatom-dominated EOF mode accompanies depleted surface nutrients and warmer surface temperatures than those for the first mode. Continued depletion of nutrients and stabilization of the water column (Table 3) leads to the oligotrophic-stratified, dinoflagellate-dominated third stage or EOF mode. *Goodman et al.* [1984] found similar sets of assemblages in a PCA analysis of phytoplankton abundances from further south in the Southern California Bight, with the first two significant axes dominated by different forms of upwelling-favored diatoms and a third axis dominated by dinoflagellates during nonupwelling conditions. The short duration of their study, however, precluded any observations of seasonal or interannual changes in the dynamics of these plankton communities.

4.2. Interannual Variability in Community Structure

[37] Our analysis reveals an apparent shift in the pattern of phytoplankton species succession within the SBC between 1998 and 2003. Large diatom blooms are absent from the first three years of the time series while the extreme negative amplitudes for the diatom mode are in fact more frequent from 1998 to 2001 than from 2002 to 2003 (Figure 6a). This trend is clearly observed in the plot of mean fucoxanthin for each bloom period (Figure 9) which shows a twofold increase in the magnitude of diatom pigment concentrations between the first 3 years of the time series and the last 2 years. Interestingly, this shift toward more intense diatom blooms coincided with spring bloom communities dominated by toxigenic species of the pennate diatom, *Pseudo-nitzschia*. Elevated domoic acid concentrations during a large *Pseudo-nitzschia* bloom in May 2003, possibly induced by Si limitation, caused significant marine mammal deaths in the SBC in May 2003 [*Anderson et al.*, 2006]. In the analysis presented here, the prevalence of the diatom-dominated, upwelling mode in the years after 2001 is also associated with depleted silicic acid concentrations, increasing wind speeds (Table 2), and a possible increase in upwelling intensity as seen in an EOF decomposition of physical and chemical variables for the same time period (D. A. Siegel et al., A time series assessment of sediment plumes and phytoplankton blooms in the Santa Barbara Channel, California, manuscript in preparation, 2008). As strong westerly winds into the SBC drive the vertical

Figure 7. The average phytoplankton community structure for surface samples at the top 3% extreme amplitudes for the first four EOF modes represented as (a) mixed assemblage, (b) diatom bloom, (c) dinoflagellate bloom, (d) transition state when nanoplankton dominate, and (e) transition state when picoplankton dominate. Error bars represent 1 standard deviation. Traditional chemotaxonomic, size class groupings and the CHEMTAX approach (Table 1) show good agreement with one another and with their respective EOF pigment modes (see Figure 4).

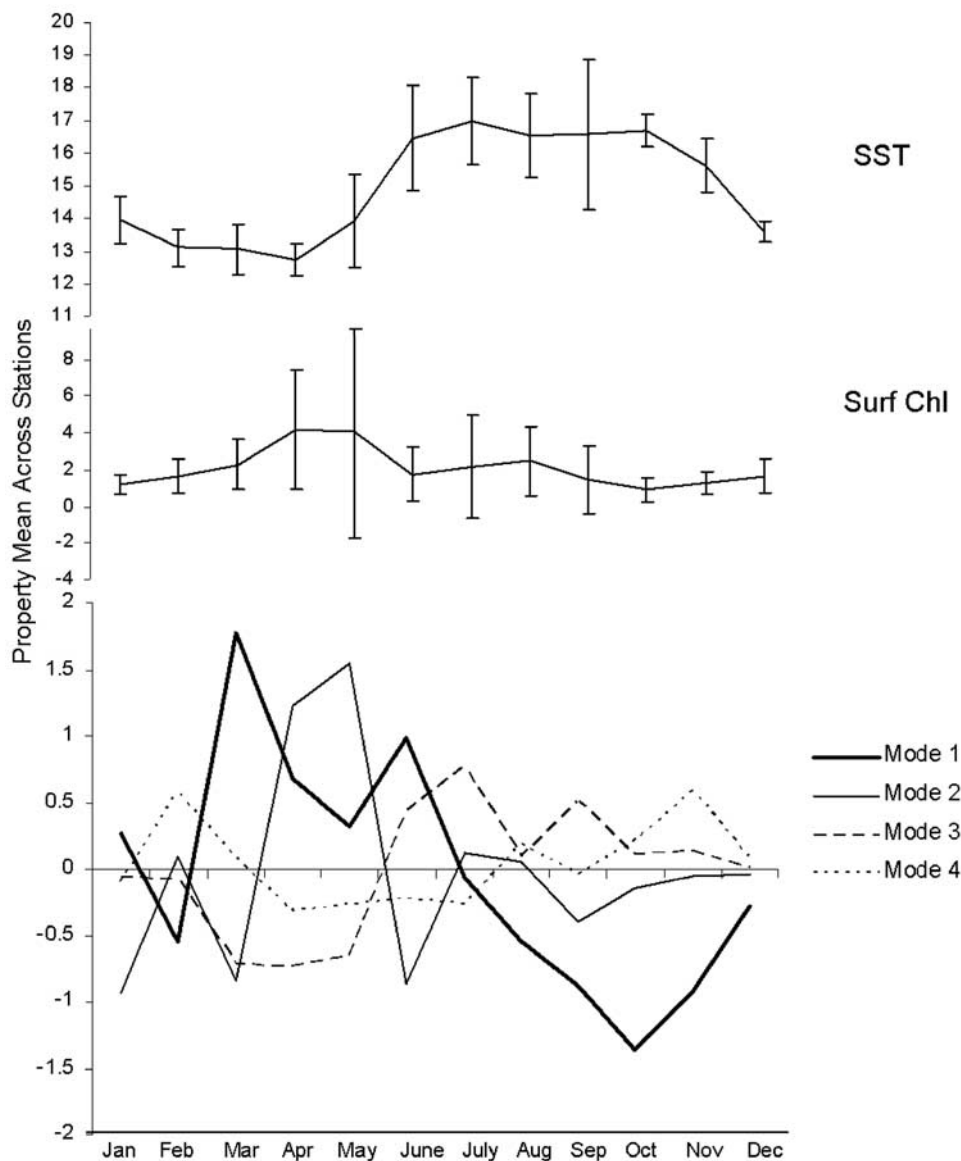


Figure 8. Monthly mean modal amplitudes for the four dominant EOF modes (averaged across all stations and years) are plotted with the corresponding monthly means for SST and surface chlorophyll *a* (error bars are standard deviation).

displacement of bottom waters over the continental shelf, this upwelling of bottom sediments should serve to resuspend resting spores and cysts [Garrison, 1981], an important mechanism for the initiation of diatom blooms, and perhaps even more so for blooms of the potentially toxic *Pseudo-nitzschia* spp. [Trainer *et al.*, 2000].

[38] The increase in the frequency of intense diatom blooms in 2002 and 2003 is matched by a decline in the frequency and intensity of dinoflagellate blooms (Mode 3, Figure 6) that were prevalent in summer during the first 3.5 years of the study. Dinoflagellate blooms increased in magnitude between 1999 and 2001 and then declined precipitously in 2002 when diatom blooms first intensified (Figure 9). This transition may represent a regime shift from a system that favors dinoflagellates to one with large diatom blooms; however, this change may also be influenced by

undersampling of the most nearshore region where dinoflagellates often occur in great abundance. Dinoflagellate blooms have certainly been recorded in tidal zones along the mainland of the Southern California Bight [Venrick, 1998] and may remain isolated there when upwelling-favorable conditions prevail in the middle of the channel [Otero and Siegel, 2004].

[39] During a recent dinoflagellate bloom event in 2004 that coincided with a late summer cruise by the SBC-LTER project, channel-wide distributions of peridinin show pigment peaks very close to shore and westward of the PnB transect (data not shown). This synoptic view suggests that, indeed, in years with reduced dinoflagellate abundance in the SBC, seasonal increases in dinoflagellate abundance may have actually been maintained nearshore but out of sampling range of the PnB program. Summer transitions to

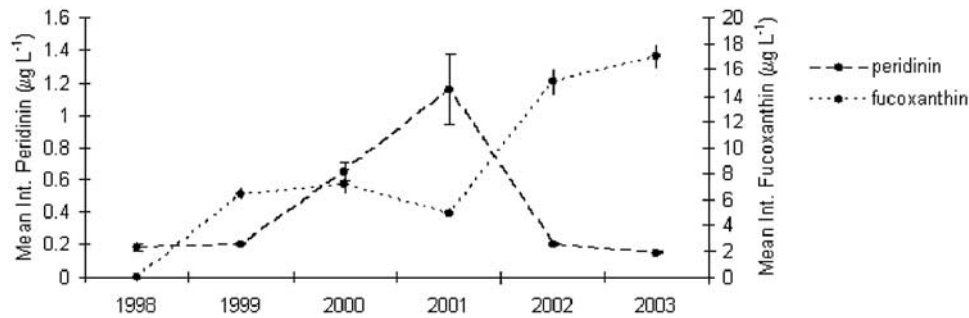


Figure 9. Mean surface fucoxanthin and peridinin concentrations are plotted for the bloom periods March–June and June–September, respectively, to illustrate the change in diatom and dinoflagellate bloom magnitudes between years (error bars denote standard deviation).

dinoflagellate dominance may not always be channel-wide, particularly during years with frequent diatom blooms. This sort of horizontal heterogeneity may be further maintained by the presence of midchannel mesoscale eddies during spring and summer [Harms and Winant, 1998] that are known to retain surface phytoplankton blooms via convergence [Anderson et al., 2006].

[40] Earlier in the spring of 2004, we also observed a nearshore bloom of the ‘red tide’ dinoflagellate, *Lingulodinium polyedrum* in the SBC, a species favored by stratified, calm surface waters [Sullivan et al., 2003; Juhl and Latz, 2002] and that interestingly dominated the third PCA axis in the study by Goodman et al. [1984]. It is thus important to note that the contribution by 19'-BF and violaxanthin to the variance of the dinoflagellate EOF mode could possibly be due to the presence of heterotrophic and/or red-tide forming dinoflagellates, such as *L. polyedrum*, which are known to contain nano- and pico-plankton pigments in their endosymbionts. For example, the pigments 19'-BF, 19'-HF, and fucoxanthin have all been found in isolated populations of *Gymnodinium* spp. [e.g., Bjornland et al., 2003], a group of potentially toxic species that do often occur in the SBC phytoplankton community [Venrick, 1998; C. Anderson, unpublished data, 2004]. Furthermore, there are interesting similarities in the shape of the peridinin and 19'-BF distributions (Figures 3b and 3c) during summer dinoflagellate blooms that may be evidence for the simultaneous presence of 19'-BF and peridinin in some members of the dinoflagellate assemblage.

4.3. Forcing From Climate Oscillations

[41] The time series of pigments analyzed here misses the majority of the 1997–1998 El Niño event, however, we did capture the transition to the 1999–2000 La Niña, allowing for some interpretation of remote forcing on phytoplankton succession. Results from an earlier and overlapping time series of satellite-derived phytoplankton bloom indices in the SBC suggest that ENSO events affect mean chlorophyll levels to a lesser degree than does local seasonal variability [Otero and Siegel, 2004]. This is observed during the La Niña year of 1999 when temperature, salinity, and nitrate distributions show pronounced upwelling-related anomalies [Otero and Siegel, 2004] during the winter and spring, but relatively weak increases in chlorophyll concentrations (Figure 2). Moreover, time series of nitrate, fucoxanthin,

and the diatom/upwelling EOF mode 2 do not reveal a particularly dramatic response from diatoms to these elevated surface nitrate concentrations in the early spring of 1999. In contrast, the amplitude functions for the first and fourth EOF modes during the spring of 1999 are at the upper 3% extreme of the amplitude range (Figures 5 and 6), with especially strong expression of the haptophyte-driven, nano-plankton phase of mode 4 throughout 1999 (Figure 6). In fact, the majority of the interannual variability for both the nano- and pico-phytoplankton stages of the fourth EOF mode appears driven by this La Niña event which ended in fall 2000.

[42] Otero and Siegel [2004] suggest that strengthening of the along-channel pressure gradient in the spring of 1999 advected oligotrophic waters from the south into the SBC, thereby reducing the availability of nutrients to phytoplankton and perhaps explaining the suppressed diatom response and greater abundance of nano- and pico-plankton. The inverse relationship between the ENSO/SOI index and the diatom-driven EOF mode (Tables 1 and 2) is also attributable to this apparent absence of an extensive diatom bloom during La Niña spring conditions. The shift after 2001 to years with large diatom blooms is interesting in light of the significant, negative correlation between the SOI index and dinoflagellate abundance (Table 1, mode 3) which points to ENSO-like conditions during the dinoflagellate bloom events of 1998, 2000, and 2001. Much of the variance of the dinoflagellate mode is also due to fluctuations in the 19'-BF containing crysophyte (or heterotrophic dinoflagellate) population (Figures 4 and 7c) which exhibits only slight interannual variability (Figure 3c) over the study period, and which unlike the haptophytes and cyanobacteria, does not appear to be remotely influenced.

5. Conclusions

[43] We have shown that four distinct phytoplankton assemblages dominate the variability in surface phytoplankton biomass and community structure in the SBC. These assemblages generally represent end points in a constantly changing, heterogeneous environment defined by a complex hydrography. Within this complexity, we found a surprising degree of resource partitioning between the dominant assemblages, whereby there is little temporal or spatial overlap in their extreme episodes (Figure 6). Significant

associations between the phytoplankton species assemblage and local forcings point to a distinct set of conditions that select for dominance by each of the modes. These range from the upwelling-driven diatom blooms to the stratification requirements for dinoflagellates and picophytoplankton. On longer timescales, it appears that forcing by ENSO may further control selection of the dominant assemblages with a recent shift toward larger diatom blooms. The overall resemblance of the different flagellate, diatom, and dinoflagellate-dominated states to stages of phytoplankton succession canonized by *Margalef* [1962], *Smayda* [1963], and others is remarkable considering the unique, regional circulation of the SBC. Should the occurrence of these well-defined assemblages and the conditions that locally select for them remain stable, we might be able to apply this knowledge to regional assessments of primary production and biogeochemistry from satellite observations.

Appendix A

[44] The relative chlorophyll contributions of eight common classes of phytoplankton were calculated using values for the pigment: chlorophyll-*a* ratio matrix recommended by CSIRO labs and SCOR-UNESCO [Mackey *et al.*, 1997; Jeffrey and Wright, 2006]. These literature values serve as approximations for the local species pigment ratios, though if available, laboratory values for the area are always preferable. Owing to the prominent role of prasinoloxanthin in driving pigment variability in the EOF analysis, pigment ratios for “Type 3” prasinophytes were used since this group contains a higher prasinoloxanthin:chlorophyll-*a* ratio than the other two groups [Mackey *et al.*, 1997] and only small amounts of lutein [Jeffrey and Wright, 2006]. Pigment ratios for the haptophytes (also “Type 3”) were chosen to represent the coccolithophorid prymnesiophyte algae rather than the *Phaeocystis*-like prymnesiophytes which have not been reported in abundance for the SBC [Venrick, 1998] (also C. Anderson, personal observation, 2003–2004). The Chrysophyte class represents both “Type 2” silicoflagellates (Dictyophyceae) and “Type 2” picoplanktonic pelagophytes [Jeffrey and Wright, 2006; Mackey *et al.*, 1997]. All other pigment ratios are mean SCOR/UNESCO values measured from representatives of each class [Mackey *et al.*, 1997] and are assumed here to be best approximations for SBC flora (Table 1). Mackey *et al.* [1996] and others [e.g., Lohrenz *et al.*, 2003] underscore the need to pool samples by depth to eliminate error caused by irradiance effects on pigment concentrations. In our analysis, we avoid biases across depths by applying CHEMTAX only to surface or near-surface samples at individual sampling stations and time points.

[45] **Acknowledgments.** This study was supported by NASA, NOAA, Channel Islands National Marine Sanctuary, and NSF support of the Plumes and Blooms (NASS-00201) and Santa Barbara Coastal LTER projects (OCE 9982105). The authors are much indebted to the many dedicated Plumes and Blooms technicians and graduate students, in particular: Olga Polyakov, Deborah Fernamburg, David Menzies, David Court, Deirdre Toole, Tihomir Kostadinov, and Chantal Swan. Many thanks go to Jason Perl and Chuck Trees of SDSU for conducting the HPLC phytoplankton pigment analyses and for their support by NASA. We would also like to thank the crew of the R/V *Shearwater* for their hard work every month. This research is part of the Ph.D. dissertation of C. Anderson,

who is supported by a NASA Earth System Science Graduate Fellowship (06-ESSF-06R-12).

References

- Allen, W. E. (1922), Observations on surface distribution of marine diatoms between San Diego and Seattle, *Ecology*, **3**, 140–145.
- Anderson, C. R., et al. (2006), Circulation and environmental conditions during a toxigenic *Pseudo-nitzschia australis* bloom in the Santa Barbara Channel, California, *Mar. Ecol. Prog. Ser.*, **327**, 119–133.
- Balch, W. M., and C. R. Byrne (1994), Factors affecting the estimate of primary production from space, *J. Geophys. Res.*, **99**, 7555–7570.
- Beers, J. R. (1986), Organisms and the food web, in *Plankton Dynamics of the Southern California Bight*, edited by R. W. Eppley, pp. 84–175, Springer, New York.
- Bidigare, R. R., et al. (2003), HPLC phytoplankton pigments: sampling, laboratory methods, and quality assurance procedures, in *Biogeochemical and Bio-optical Measurements and Data Analysis Protocols*, edited by J. L. Mueller *et al.*, pp. 5–14, NASA, Washington, D.C.
- Bjornland, T., et al. (2003), Carotenoids of the Florida red tide dinoflagellate *Karenia brevis*, *Biochem. Syst. Ecol.*, **31**, 1147–1162.
- Breaker, L. C., et al. (2003), A curious relationship between the winds and currents at the western entrance of the Santa Barbara Channel, *J. Geophys. Res.*, **108**(C5), 3132, doi:10.1029/2002JC001458.
- Brzezinski, M. A., and D. M. Nelson (1989), Seasonal changes in the silicon cycle within a Gulf Stream warm-core ring, *Deep Sea Res., Part I*, **36**, 1009–1030.
- Cembella, A. D., et al. (2002), The toxigenic marine dinoflagellate *Alexandrium tamarense* as the probable cause of mortality of caged salmon in Nova Scotia, *Harmful Algae*, **1**, 313–325.
- Chen, C.-S., and D.-P. Wang (2000), Data assimilation model study of wind effects in the Santa Barbara Channel, *J. Geophys. Res.*, **105**, 22,003–22,013.
- Claustre, H., et al. (1997), Sources of variability in the column photosynthetic cross section for Antarctic coastal waters, *J. Geophys. Res.*, **102**, 25,047–25,060.
- Doblin, M. A., et al. (1999), Growth and biomass stimulation of the toxic dinoflagellate *Gymnodinium catenatum* (Graham) by dissolved organic substances, *J. Exp. Mar. Biol. Ecol.*, **236**, 33–47.
- Dugdale, R. C., et al. (1990), Realization of new production in coastal upwelling areas: A means to compare relative performance, *Limnol. Oceanogr.*, **35**, 822–829.
- Emery, W. J., and R. E. Thomson (1997), *Data Analysis Methods in Physical Oceanography*, Pergamon, New York.
- Garrison, D. L. (1981), Monterey Bay Phytoplankton. II. Resting spore cycles in coastal diatom populations, *J. Plankton Res.*, **3**, 137–156.
- Gieskes, W. W. C., et al. (1988), Monsoonal alteration of a mixed and a layered structure in the phytoplankton of the euphotic zone of the Banda Sea (Indonesia): A mathematical analysis of algal fingerprints, *Neth. J. Sea Res.*, **22**, 123–137.
- Goodman, D., et al. (1984), Summer phytoplankton assemblages and their environmental correlates in the Southern California Bight, *J. Mar. Res.*, **42**, 1019–1049.
- Guzman-Bustillos, J., et al. (1995), Specific phytoplankton signatures and their relationship to hydrographic conditions in the coastal northwestern Mediterranean Sea, *Mar. Ecol. Prog. Ser.*, **124**, 247–258.
- Harms, S., and C. D. Winant (1998), Characteristic patterns of the circulation in the Santa Barbara Channel, *J. Geophys. Res.*, **103**, 3041–3065.
- Jeffrey, S. W., and S. W. Wright (1994), Photosynthetic pigments in the Haptophyta, in *The Haptophyte Algae*, edited by J. C. Green and B. S. C. Leadbeater, pp. 111–132, Clarendon Press, Oxford, UK.
- Jeffrey, S. W., and S. W. Wright (2006), Photosynthetic pigments in marine microalgae: Insights from cultures and the sea, in *Algal Cultures, Analogues of Blooms and Applications*, edited by D. V. Subba Rao, pp. 33–90, Sci. Publ., Enfield, N.H.
- Juhl, A. R., and M. I. Latz (2002), Mechanisms of fluid shear-induced inhibition of population growth in a red-tide dinoflagellate, *J. Phycol.*, **38**, 683–694.
- Knap, A. H., et al. (1993), *BATS Methods Manual*, U.S. JGOFS Plann. Off., Woods Hole, Mass.
- Kostadinov, T. S., et al. (2007), Ocean color observations and modeling for an optically complex site: Santa Barbara Channel, California, USA, *J. Geophys. Res.*, **112**, C07011, doi:10.1029/2006JC003526.
- Letelier, R. M., et al. (1993), Temporal variability of phytoplankton community structure based on pigment analysis, *Limnol. Oceanogr.*, **38**, 1420–1437.
- Lohrenz, S. E., et al. (2003), Variations in phytoplankton pigments, size structure and community composition related to wind forcing and water mass properties on the North Carolina inner shelf, *Cont. Shelf Res.*, **23**, 1447–1464.

- Lynn, R. J., and J. J. Simpson (1987), The California Current system: The seasonal variability of its physical characteristics, *J. Geophys. Res.*, *92*, 12,947–12,966.
- Mackey, M. D., et al. (1996), CHEMTAX—A program for estimating class abundances from chemical markers: Application to HPLC measurements of phytoplankton, *Mar. Ecol. Prog. Ser.*, *144*, 265–283.
- Mackey, M. D., et al. (1997), CHEMTAX user's manual: A program for estimating class abundances from chemical markers—Application to HPLC measurements of phytoplankton pigments, *Rep.* *229*, 47 pp., CSIRO Mar. Lab., Hobart, Tasmania, Australia.
- Mantyla, A. W., et al. (1995), Primary production and chlorophyll relationships, derived from ten years of CALCOFI measurements, *CalCOFI Rep.* *36*, pp. 159–166, Calif. Coop. Oceanic Fish. Invest., La Jolla.
- Margalef, R. (1962), Succession in marine populations, *Adv. Front. Plant Sci.*, *2*, 137–188.
- Margalef, R. (1978), Life-forms of phytoplankton as survival alternatives in an unstable environment, *Oceanol. Acta*, *1*, 493–509.
- McPhee-Shaw, E. E., et al. (2007), Mechanisms for nutrient delivery to the inner shelf: Observations from the Santa Barbara Channel, *Limnol. Oceanogr.*, *52*, 1748–1766.
- Mertes, L. A. K., and J. A. Warrick (2001), Measuring flood output from 110 coastal watersheds in California with field measurements and SeaWiFS, *Geology*, *29*, 659–662.
- Moline, M. A., and B. B. Prezelin (1996), Long-term monitoring and analyses of physical factors regulating variability in coastal Antarctic phytoplankton biomass, in situ productivity and taxonomic composition over subseasonal, seasonal and interannual time scales, *Mar. Ecol. Prog. Ser.*, *145*, 143–160.
- Mueller, J. L., and R. W. Austin (1995), Ocean optics protocols for SeaWiFS validation, *NASA Tech. Memo*, *104566*, 67 pp.
- Mullin, M. M. (1986), Spatial and temporal scales and patterns, in *Plankton Dynamics of the Southern California Bight*, edited by R. W. Eppley, pp. 216–273, Springer, New York.
- Oey, L.-Y., et al. (2001), "Upwelling" and "cyclonic" regimes of the near-surface circulation in the Santa Barbara Channel, *J. Geophys. Res.*, *106*, 9213–9222.
- Orwig, D. L. (1978), An ecological study of the phytoplankton and microzooplankton of two inshore areas in the Santa Barbara Channel, Ph.D. dissertation, Univ. of Calif., Santa Barbara.
- Otero, M. P., and D. A. Siegel (2004), Spatial and temporal characteristics of sediment plumes and phytoplankton blooms in the Santa Barbara Channel, *Deep Sea Res., Part II*, *51*, 1129–1149.
- Schlüter, L., et al. (2000), The use of phytoplankton pigments for identifying and quantifying phytoplankton groups in coastal areas: testing the influence of light and nutrients on pigment/chlorophyll *a* ratios, *Mar. Ecol. Prog. Ser.*, *192*, 49–63.
- Siegel, D. A., et al. (1990), Meridional variations of the springtime phytoplankton community in the Sargasso Sea, *J. Mar. Res.*, *48*, 379–412.
- Smayda, T. J. (1963), Succession of phytoplankton, and the ocean as an holocoenotic environment, in *Symposium on Marine Microbiology*, edited by C. H. Oppenheimer, pp. 260–274, Thomas, Springfield, Ill.
- Sullivan, J. M., et al. (2003), Small-scale turbulence affects the division rate and morphology of two red-tide dinoflagellates, *Harmful Algae*, *2*, 183–199.
- Trainer, V. L., et al. (2000), Domoic acid production near California coastal upwelling zones, June 1998, *Limnol. Oceanogr.*, *45*, 1818–1833.
- Venrick, E. L. (1998), Spring in the California Current: The distribution of phytoplankton species, April 1993 and April 1995, *Mar. Ecol. Prog. Ser.*, *167*, 73–88.
- Vidussi, F., et al. (2001), Phytoplankton pigment distribution in relation to upper thermocline circulation in the eastern Mediterranean Sea during winter, *J. Geophys. Res.*, *106*, 19,939–19,956.
- Warrick, J. A., et al. (2004), Dispersal forcing of southern California river plumes, based on field and remote sensing observations, *Geo Mar. Lett.*, *24*, 46–52.
- Winant, C. D., et al. (1987), Moored wind, temperature, and current observations made during Coastal Ocean Dynamics Experiments 1 and 2 over the northern California continental shelf and upper slope, *J. Geophys. Res.*, *92*, 1569–1604.
- Winant, C. D., et al. (2003), Characteristic patterns of shelf circulation at the boundary between central and southern California, *J. Geophys. Res.*, *108*(C2), 3021, doi:10.1029/2001JC001302.

C. R. Anderson, NOAA, ESSIC/CICS, University of Maryland, College Park, MD 20742, USA. (clarissa@umd.edu)

M. A. Brzezinski, Marine Science Institute and the Department of Ecology, Evolution, and Marine Biology, University of California, Santa Barbara, CA 93106, USA.

N. Guillocheau and D. A. Siegel, Institute for Computational Earth System Science, University of California, Santa Barbara, CA 93106, USA.